Geometrical methods for analyzing the optimal management of tipping point dynamics

Wagener, F.

DOI
10.1111/nrm.12258

Publication date
2020

Document Version
Final published version

Published in
Natural Resource Modeling

Received: 2 November 2019 | Accepted: 14 January 2020

DOI: 10.1111/nrm.12258

Natural Resource Modeling WILEY

Geometrical methods for analyzing the optimal management of tipping point dynamics

Florian Wagener

Amsterdam School of Economics, Universiteit van Amsterdam, Amsterdam, The Netherlands

Correspondence
Florian Wagener, Universiteit van Amsterdam, Roetersstraat 11, 1018 WB Amsterdam, The Netherlands.
Email: f.o.o.wagener@uva.nl

Abstract

Natural resources are not infinitely resilient and should not be modeled as being such. Finitely resilient resources feature tipping points and history dependence. This paper provides a didactical discussion of mathematical methods that are needed to understand the optimal management of such resources: viscosity solutions of Hamilton–Jacobi–Bellman equations, the costate equation and the associated canonical equations, exact root counting, and geometrical methods to analyze the geometry of the invariant manifolds of the canonical equations.

Recommendations for Resource Managers

- Management of natural resources has to take into account the possible breakdown of resilience and induced regime shifts.
- Depending on the characteristics of the resource and on its present and future economic importance, either for all initial states the same kind of management policy is optimal, or the type of the optimal management policy depends on the initial state.

- Modeling should reflect the finiteness of the data.

KEYWORDS

dynamic programming, exact rootfinding, Hamilton–Jacobi–Bellman equation, indifference points, invariant manifolds, state–costate equations, trappingregions, viscosity solutions

1 | INTRODUCTION

The present article is based on my lecture "Geometry and the Economic Impact of Ecological Systems with Tipping Points," which I gave at the 2019 World Conference on Natural Resource Modelling in Montréal, Canada. Then and now, my aim is to show how modern mathematical methods can be used to analyze the management of natural resources. The article is aimed at nonspecialists that want to understand dynamic optimization methods to a point where they might be able to apply them to their own models, but who are willing to take on trust a number of results that are well-documented in the literature.

Natural systems are resilient: momentarily perturbed from a steady state by some external stress, these systems return to their original state, or, if the stress is permanent, settle to a new state. Economic models of natural resources often assume that natural systems are infinitely resilient, which is defensible if stresses are small.

Real natural systems are not infinitely resilient. Under large stresses, resilience breaks down and the system tips over to a new regime: corals bleach, lakes eutrophy, ice-sheets melt. Beyond the tipping point, the negative feedback mechanism stabilizing the old regime is less powerful than the positive feedback mechanism forcing the shift to the new. In this context "negative" and "positive" do not imply value judgments: they are technical terms indicating that small disturbances decay or grow over time at a negative or a positive rate.

Positive feedbacks go hand in hand with multiple possible steady states or more complex forms of long-term behavior. Mathematical models describing such situations are nonlinear and usually not solvable by quadratures. In particular, if economic activities stress a natural resource significantly, computing an optimal management plan is a hard mathematical problem.

In the following, I shall analyze a situation featuring positive feedbacks and multiple steady states to show how much may be done, and may be done rigorously, by geometrical methods that are relatively accessible. In particular, numerical methods will only serve to produce illustrations. I shall, however, admit computer-assisted proofs of statements that are tedious to prove by hand.

The dynamics of systems that can switch between several regimes always has a qualitative dimension. Before determining the detailed management plan, it is already of interest to know whether optimal management will steer the system to one regime or another. The latter question demands less detail of the solution, is therefore more likely to be answered, and will be our main concern. We shall want to know whether the optimal plan exists and what the qualitative characteristics of the resulting system dynamics are if the optimal plan is implemented.

The existence of solutions to the optimal management problem will be shown by dynamic programming. Since the advent of viscosity theory in the 1980's, this method has been promoted, like Heaviside calculus before it, from "heuristically useful but not quite correct" to "fully rigorous."

A perceived defect of viscosity theory is that it requires compact action spaces and bounded cost functions, although these requirements are being weakened (Bardi & Capuzzo-Dolcetta, 2008). This apparent defect actually has a beneficial effect, as it forces us to acknowledge that the available information, which is always finite, only allows us to make assumptions for bounded parameter ranges. Infinite quantities should only be admitted when this simplifies an aspect of the problem. This is not the case here: unbounded action spaces or state spaces create additional mathematical difficulties. It is different for the time interval: this is often chosen to run to infinity, to relieve us from modeling what happens at the end of the planning horizon.

The "economically reasonable" solution to the dynamic programming problem will be constructed using methods from the geometric theory of dynamical systems. A general result ensures that the solution obtained is the viscosity solution. From viscosity theory, we use the basic results, valid in the present setting, that the value function is a viscosity solution and that viscosity solutions are unique. They allow us to verify that the economically reasonable solution is indeed the value function of the problem.

Only systems with one-dimensional state spaces are considered. This is done to keep technical complexity to a minimum, and also because these systems are well understood and can be illustrated by two-dimensional diagrams. Both the solution philosophy and the solution methods can be generalized to higher dimensions, with the exception of results that rely on the Poincaré–Bendixson theorem.

The second section introduces a class of optimal management problems and sketches the dynamic programming approach that leads to formulating the Hamilton–Jacobi–Bellman differential equation for the value of these problems. The third section indicates three main technical difficulties that have to be overcome to arrive at a solution. First, the classical solution notion is too narrow and has to be enlarged; second, the equation is implicit and therefore inconvenient to work with; and, third, closed form solutions are in general impossible to obtain. The section discusses methods to overcome these difficulties. The fourth section illustrates these methods in the situation of the optimal management of a lake. Typically nonclassical solutions feature indifference points: these are states at which more than one policy is optimal. The final section gives an—incomplete—overview of the literature of optimal management problems with nonclassical value functions.

2 | MANAGING NATURAL RESOURCES WITH TIPPING POINTS

This section introduces a class of natural resources whose natural decay rate is negatively affected when the resource is stressed. The analysis of the optimal management problem of such resources is the main theme of this article.

2.1 | System evolution

The state of the natural resource is described by the real quantity $x(t)$. I shall take a lake ecosystem as my standard example, but other interpretations are possible. In the lake model, the state is the stock of phosphorus in the water column, a nonnegative quantity.

The state is affected by actions $a(t)$ of the manager, which are also real quantities. For the lake, this is the 'loading' of the lake with phosphorus, which is intended to fertilize the fields surrounding the lake, but whose excess is washed into the lake by rainfall.

As a general rule, I shall use "state" and "action" when developing theoretical relationships, and "pollution stock" and "loading" when discussing specifically pollution problems.

The differential equation

$$\dot{x} = f(x, a), \quad x(0) = y \tag{1}$$

describes the time evolution of the state, with y denoting its initial value. The time argument t of the variables x and a is suppressed, and $\dot{x}$ indicates differentiation of x with respect to time.

I assume particularly

$$f(x, a) = a - g(x), \tag{2}$$

that is, the natural decay $g(x)$ depends only on the state level x.

Two decay functions are illustrated in Figure 1. The dashed line corresponds to linear decay

$$g(x) = bx. \tag{3}$$

Under time-independent actions a, the system settles at a steady state level $x = a/b$. Such a system is infinitely resilient, as the steady state level varies continuously with the action.

The "lake" decay

$$g(x) = bx - \frac{x^2}{1 + x^2} \tag{4}$$

models resilience loss (Carpenter & Cottingham, 1997; Mäler, Xepapadeas, & de Zeeuw, 2003), for here the steady state is a discontinuous function of the loading. This is illustrated in Figure 2: for an initially unpolluted resource and small loadings, the steady state stock x increases almost linearly with a, as in Figure 2a. At the local maximum of the decay function, the system loses its resilience. If the loading increases past this value, the steady state jumps

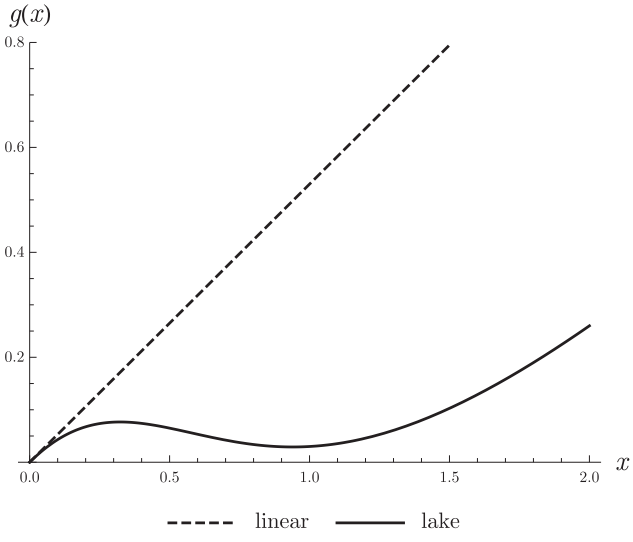

FIGURE 1 Linear and lake decay functions

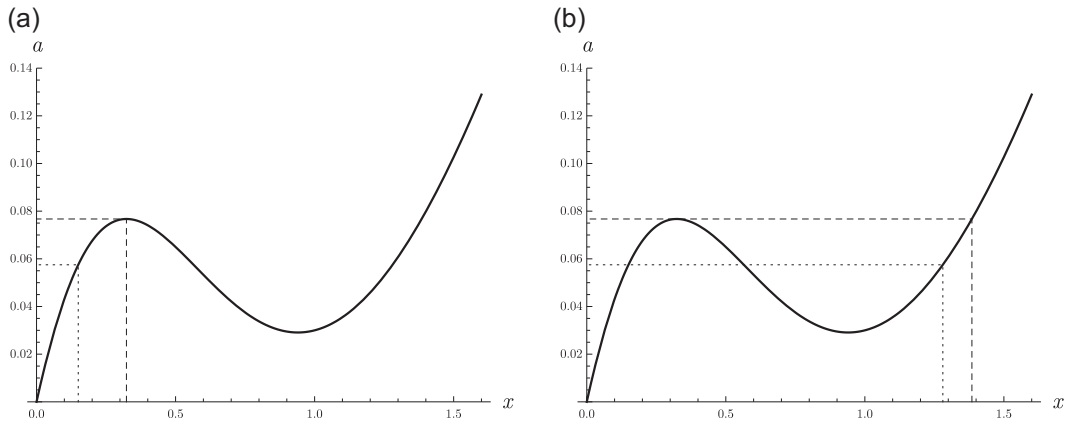

FIGURE 2 Tipping point and hysteresis effect ($b = 0.53$). (a) Before tipping and (b) after tipping

discontinuously to a much higher value, as in Figure 2b. That figure also shows that decreasing the loading to its former value does not restore the pollution stock to its former level: it remains high.

2.2 | Economic valuations

For an ecologist, economic activities stress natural resources; for an economist, resources provide services. A lake provides freshwater, fishing, recreation, but it can also serve as a waste dump. To decide about how a natural resource should be best used, these services have to be valued.

The cost flow of pollution is modeled as the shortfall

$$-cx^2$$

of the income from an entirely unpolluted lake.

Phosphorus is a major pollutant of lakes, because it stimulates the growing of algae. It is also an important artificial fertilizer used in agriculture. In the economic lake literature, its benefits are modeled as

$$\log a.$$

Both lake and agriculture generate benefits. We assume a decision maker that regulates the use of artificial fertilizer, with the objective to maximize the discounted future benefits

$$J(a; s, y) = \int_s^\infty \mathrm{e}^{-r(t-s)}(\log a - cx^2)dt$$

that can be obtained at time s, if the initial stock level is $x(s) = y$.

2.3 | The principle of optimality

The mathematical problem of the decision maker is to choose an action schedule a from a certain set $\mathscr{A}$ of admissible schedules to maximize objective J subject to the dynamic evolution

$$\dot{x} = f(x, a), \quad x(s) = y. \tag{5}$$

At each time s, a value

$$V(s, y) = \sup_{a \in \mathscr{A}} J(a; s, y) = \sup_{a \in \mathscr{A}} \int_s^\infty \mathrm{e}^{-r(t-s)} \ell(x, a) dt \tag{6}$$

is associated to the stock level y. The dynamic programming approach consists in characterizing this value as the solution of a partial differential equation, the Hamilton–Jacobi–Bellman equation, and expressing optimal actions in terms of its derivatives.

Making sufficiently strong assumptions, this equation can be derived readily. Assume first that the supremum in (6) is taken for an admissible action schedule $a^*(t)$ with corresponding state evolution $x^*(t)$. Splitting the time interval $[s, \infty)$ in the subintervals $[s, s_1)$ and $[s_1, \infty)$ yields then

$$V(s, y) = \int_s^{s_1} \mathrm{e}^{-r(t-s)} \ell(x^*, a^*) dt + \mathrm{e}^{-r(s_1-s)} V(s_1, x^*(s_1)). \tag{7}$$

For if equality did not hold, there would be an action schedule $a(t)$ that is different from $a^*(t)$ on the time interval $[s_1, \infty)$ increasing the value. But that belies $a^*(t)$ maximizing J.

Dividing (7) by $s_1 - s$, rearranging terms, and taking the limit $s_1 \to s$ yields

$$-\frac{d}{ds} V(s, x^*(s)) + rV(s, x^*(s)) = \ell(x^*(s), a^*(s)). \tag{8}$$

If V is differentiable—second assumption—this relation can be written as

$$V_s(s, y) + V_y(s, y) f(y, a^*(s)) - rV(s, y) + \ell(y, a^*(s)) = 0. \tag{9}$$

For an arbitrary admissible state–action pair, Equations (7)–(9) turn into inequalities, as the realized benefit flow $\ell(x(t), a(t))$ may be suboptimal. Hence the choice $a = a^*(s)$ maximizes the left-hand side of (9), which can be written as

$$V_s(s, y) - rV(s, y) + \max_a [\ell(y, a) + V_y(s, y) f(y, a)] = 0. \tag{10}$$

Note that calendar time nowhere enters the problem: dynamics and benefits only depend on state and actions, not explicitly on time. Hence the value is independent of time, $V(s, y) = V(y)$, and after substituting x for y Equation (10) takes the form

$$-rV(x) + \max_a [\ell(x, a) + V'(x) f(x, a)] = 0. \tag{11}$$

This is the stationary Hamilton–Jacobi–Bellman or HJB equation. It expresses, net of discounting, that for an optimal choice of a the decrease

$$-V'(x)f(x,a)dt = -\frac{dV}{dx}\frac{dx}{dt}dt = -dV$$

of future benefits equals the realization

$$\ell(x,a)dt$$

of present benefits. Equation (11) holds at points where the value function is differentiable, if an optimizing action schedule exists. However, there are situations, important ones, where the value function is not differentiable. If we want the Hamilton–Jacobi–Bellman equation to describe these situations, we have to extend its meaning.

3 | THEORY OF HAMILTON–JACOBI–BELLMAN EQUATIONS

The compact way of writing the Hamilton–Jacobi–Bellman equation is

$$rV(x) - H(x, V'(x)) = 0,$$

where

$$H(x,p) \stackrel{\text{def}}{=} \max_a [\ell(x,a) + pf(x,a)]. \tag{12}$$

For future use, note a particular feature of H. The expression in square brackets is a family, parametrized by x and a, of linear functions

$$p \mapsto \ell(x,a) + pf(x,a).$$

The pointwise maximum of such a family is convex, therefore $H(x,p)$ is convex in its second argument.

3.1 | Three difficulties

Working with Hamilton–Jacobi–Bellman equations present three technical difficulties.

The first difficulty we already have alluded to: the concept of the solution has to be enlarged to accommodate nondifferentiable value functions. Second, Hamilton–Jacobi–Bellman equations are implicit: the derivative V' is not expressed explicitly as a function of x and V, which makes the equations awkward to work with. Finally, these equations are nonlinear and it is generally impossible to obtain closed form solutions.

For each difficulty, there is an appropriate mathematical tool. A nondifferentiable value function may be a viscosity solution of the Hamilton–Jacobi–Bellman equation. Crandall and

Lions (1983), who developed this solution concept, showed, given suitable hypotheses, the value function to be the unique viscosity solution of the Hamilton–Jacobi–Bellman equation.

Implicit differential equations have been analyzed since the first days of calculus. The core idea is to take the derivative of the unknown function, the costate, as fundamental object. This works particularly well for the Hamilton–Jacobi–Bellman equation, as differentiation with respect to the state transforms it into a first-order quasi-linear equation of the costate. This equation may still have singularities, but these can be dealt with by a second transformation, resulting in the state–costate equations.

These equations form a regular, explicit, nonlinear dynamical system. Poincaré started the development of systematic methods to derive qualitative properties of the solutions directly from the defining equations (Poincaré, 1881, 1882, 1885, 1886).

The remainder of this section discusses viscosity theory and the canonical equations. The next section analyses the lake management problem using Poincaré's geometrical methods.

3.2 | Viscosity theory

3.2.1 | The hedgehog problem

A nondifferentiable value function already occurs if a hedgehog wants to get off a busy street. Let $x \in [0, 1]$ be the hedgehog's position. If $x = 0$ or $x = 1$, it stands on the pavement and is safe from possible accidents. While $0 < x < 1$, it incurs the possibility of being hit by a car. It prefers not to be hit, but it does not care about where or when: the expected benefit flow is negative and constant in space and time. We normalize it to -1. The hedgehog stands initially in position y, and it can move at a speed a:

$$\dot{x} = a, \quad x(0) = y. \tag{13}$$

Movement carries an exertion cost $-a^2/4$. Let $\tau \geq 0$ be the first time the hedgehog reaches the pavement:

$$\tau = \min\{t \geq 0 \colon x(t) = 0 \text{ or } x(t) = 1\}.$$

This results in the problem to maximize

$$J(a; y) = \int_0^\tau \left(-1 - \frac{a^2}{4}\right) dt, \tag{14}$$

subject to (13). The discount rate is set to zero.

The hedgehog's Hamilton–Jacobi–Bellman equation reads as

$$0 = -H(x, V'(x)) = -\max_a \left[-1 - \frac{a^2}{4} + V'(x)a\right],$$

and it is complemented by the boundary conditions

$$V(0) = V(1) = 0,$$

as the hedgehog incurs no damage on the pavement. Note the odd way the equation is written, with a minus sign in front of the function H: this will be significant later on.

Solving for the action $a = 2V'(x)$ and substituting this into the Hamilton–Jacobi–Bellman equation reduces it to

$$0 = -H(x, V'(x)) = 1 - (V')^2, \quad V(0) = V(1) = 0. \tag{15}$$

It is intuitively clear that the reasonable solution of this equation is

$$V(x) = \begin{cases} -x, & 0 \le x \le \frac{1}{2}, \\ x - 1, & \frac{1}{2} < x \le 1, \end{cases} \tag{16}$$

which shows that the worst initial position is in the middle of the street. What is needed is a solution concept for the Hamilton–Jacobi–Bellman equation that results in this and only this solution.

Recall that an explicit first-order differential equation

$$V' = f(x, V) \tag{17}$$

defines a direction field in the (x, V)-plane, the phase plane, as at every point the value of the derivative of V is specified uniquely through (17). In contrast, our Hamilton–Jacobi–Bellman Equation (15) defines a bi-direction field, as at every point (x, V) there are the two possibilities $V' = 1$ and $V' = -1$.

Equation (15) has no everywhere differentiable solutions. For such a solution has to satisfy $V'(x) = 1$ or $V'(x) = -1$ for all x, but that is incompatible with the boundary conditions.

We might consider a function V to be a solution if it satisfies (15) almost everywhere. But then there are too many solutions, as any function satisfying the boundary conditions and whose derivative is 1 on a measurable set of measure $\frac{1}{2}$ and -1 on its complement is a solution: for instance, the function $W(x) = -V(x)$, with V as in (16), would be a solution.

The way out of this quandary is to apply an idea that originated in computational fluid dynamics. There numerical methods have great difficulties to compute the motion of non-viscous fluids, like water, as approximation errors generate spurious oscillations. The solution was to add a little "artificial viscosity," which suppressed the oscillations.

In dynamic optimization problems, a similar artifice is to add a little stochasticity to the motion: that is, we consider a slightly drunk hedgehog. Without delving here in the modeling details, this results in an additional second-order term to the Hamilton–Jacobi–Bellman equation. For the drunk hedgehog the equation reads as

$$0 = 1 - (V')^2 - \varepsilon V'', \quad V(0) = V(1) = 0 \tag{18}$$

The equation can be integrated:

$$V_\varepsilon(x) = -x + 1 + \varepsilon \log \frac{1 + e^{(2x-1)/\varepsilon}}{1 + e^{1/\varepsilon}}.$$

Taking the limit $\varepsilon \downarrow 0$ indeed selects our expected solution (16), as $V_\varepsilon(x)$ tends to $V(x)$ uniformly in x. Denote by $v(x)$ the limit of $V'_\varepsilon(x)$ as $\varepsilon \downarrow 0$. Then

$$v(x) = \lim_{\varepsilon \downarrow 0} \left(-1 + \frac{2e^{(2x-1)/\varepsilon}}{1 + e^{(2x-1)/\varepsilon}} \right) = V'(x) \quad \text{if } 0 \le x \le 1, \quad x \ne \frac{1}{2},$$

while $v\left(\frac{1}{2}\right) = 0$. Taking the zero-fluctuation limit of the stochastic problem yields the expected solution of the original Hamilton–Jacobi–Bellman equation. As the derivative of the stochastic value function converges everywhere to the derivative of the expected solution, except at $x = \frac{1}{2}$, Equation (18) implies that the second-order term $\varepsilon V''_\varepsilon(x)$ tends to 0 everywhere except at $x = \frac{1}{2}$, and $\varepsilon V''_\varepsilon\left(\frac{1}{2}\right) \to 1$. That is, the limit $V_0(x)$ solves the Hamilton–Jacobi–Bellman equation almost everywhere, and where it fails to be differentiable, at $x = \frac{1}{2}$, it at least satisfies

$$F(x, V_0(x), v(x)) = -H(x, v(x)) = 1 - v(x)^2 \ge 0.$$

It is significant that $v\left(\frac{1}{2}\right)$ is in the convex set $[v^-, v^+]$ where v^- and v^+ are the limits of V'_0 as x tends to $\frac{1}{2}$ from respectively below or above. In other words, $v\left(\frac{1}{2}\right)$ is the derivative of a function that touches the graph of $V(x)$ from below in $x = \frac{1}{2}$ and for that value of x we have $F(x, V(x), v(x)) \ge 0$.

3.2.2 | Definition of viscosity solution

The example motivates the following definition. In contrast to the example, it is formulated in terms of the original equation, without recourse to an approximating higher order equation. The formulation is for functions on the real line, but it generalizes directly to functions of several variables.

Definition 2.1. Let $\Omega \subset \mathbb{R}$ be an open set and F: $\Omega \times \mathbb{R} \times \mathbb{R}$ a continuous function. A continuous function V: $\Omega \to \mathbb{R}$ is a *viscosity supersolution* of $F(x, V(x), V'(x)) = 0$, if for every point $x_0 \in \Omega$ and every continuously differentiable function φ: $\Omega \to \mathbb{R}$ such that $\varphi(x_0) = V(x_0)$ and $\varphi(x) \le V(x)$ for $x \in \Omega$, the inequality

$$F(x_0, V(x_0), \varphi'(x_0)) \ge 0$$

holds.

A function V is a *viscosity subsolution*, if for every continuously differentiable function φ such that $\varphi(x_0) = V(x_0)$ and $\varphi(x) \ge V(x)$ for $x \in \Omega$, the inequality

$$F(x_0, V(x_0), \varphi'(x_0)) \le 0$$

holds.

A function V is a *viscosity solution*, if it is both a viscosity supersolution and a viscosity subsolution.

Formulated geometrically, if the graph of a continuously differentiable function—usually called a test function—touches the graph of V from below at a point x_0, then $F(x_0, \varphi(x_0)$,

$\varphi'(x_0)) = F(x_0, V(x_0), \varphi'(x_0))$ *over*shoots 0, and V is a *super*solution at x_0, while if the graph of φ touches from above, then $F(x_0, \varphi(x_0), \varphi'(x_0))$ *under*shoots 0, and V is a *sub*solution at x_0 (Figure 3).

Clearly, if V is differentiable at x_0, we can find test functions touching the graph of V at x_0 both from below and from above, implying that $F(x_0, V(x_0), V'(x_0)) = 0$.

3.2.3 | Relevant mathematical results

This section states the central mathematical results from the viscosity theory that will be used below in the analysis of the lake problem.

The first result states that value functions are viscosity solutions. The second states that supersolutions are larger than subsolutions everywhere. This then implies that viscosity solutions are unique and that the value function is the unique viscosity solution of the Hamilton–Jacobi–Bellman equation.

All these results hold under a number of technical assumptions. We formulate these for a situation where, unlike the hedgehog problem, there are no boundary conditions and the state space can be chosen a bounded open set. These assumptions are hypotheses for all the theorems in this section. In particular, they imply assumptions A_0–A_4 in Chapter 3 of Bardi and Capuzzo-Dolcetta (2008), where also the proofs of the results can be found.

Standing assumptions.

- *A*1. *The control set* A *is a compact subset of a finite dimensional vector space.*
- *A*2. *The space of admissible schedules* $\mathscr{A}$ *is the set of Lebesgue measurable functions* $a : [0, \infty) \to A$.
- *A*3. *The state space is a bounded open interval* $\Omega \subset \mathbb{R}$.
- *A*4. *If* $\bar{\Omega}$ *denotes the closure of* Ω, *the functions* $\ell, f \colon \bar{\Omega} \times A \to \mathbb{R}$ *are continuous, and hence bounded.*
- *A*5. *The functions* ℓ *and* f *satisfy a Lipschitz condition with respect to the first argument, that is, there is* $\mathrm{M} > 0$ *such that for all* $x, y \in \bar{\Omega}$ *and all* $a \in A$

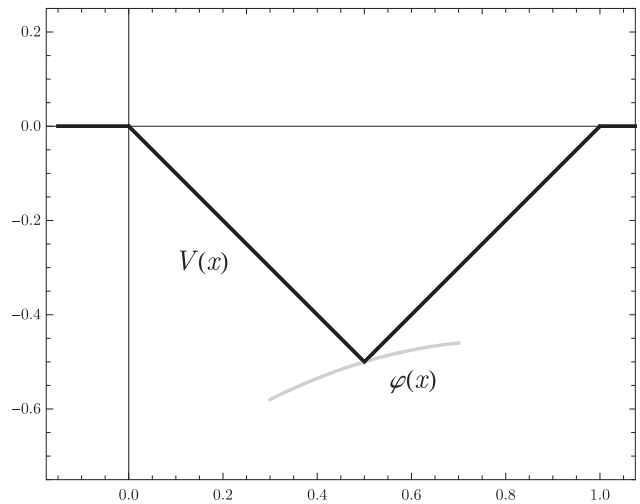

FIGURE 3 Viscosity solution $V(x)$ and test function $\varphi(x)$ touching from below

$$|\ell(x,a)-\ell(y,a)| \le M|x-y|, \quad |f(x,a)-f(y,a)| \le M|x-y|.$$

A6. *The discount rate* r *satisfies* $r>0$.

As we are discussing only autonomous optimization problems, we consider the benefit functional

$$J(a;y) = \int_0^\infty \mathrm{e}^{-rt}\ell(x,a)dt \tag{19}$$

and the evolution equation

$$\dot{x} = f(x,a), \quad x(0)=y. \tag{20}$$

The Hamilton–Jacobi–Bellman equation associated to maximizing J subject to (20) is

$$F(x,V(x),V'(x)) \stackrel{\text{def}}{=} rV(x) - H(x,V'(x)) = 0, \tag{21}$$

where H is given in (12).

Theorem 2.1. *The value function* $V(y) = \sup_{a\in\mathscr{A}} J(a;y)$ *is a viscosity solution of the Hamilton–Jacobi–Bellman Equation* (21).

Compare Bardi and Capuzzo-Dolcetta (2008, Proposition 2.8).

Theorem 2.2. *Let u, v be bounded and uniformly continuous functions such that u is a viscosity subsolution and v a viscosity supersolution of* (21). *Then* $u \le v$ *on* $\bar{\Omega}$.

Compare Bardi and Capuzzo-Dolcetta (2008, Theorem 2.12).

If there are two viscosity solutions u and v of the Hamilton–Jacobi–Bellman equation, then $u \le v$ as u is a subsolution and v a supersolution, but also $v \le u$ as v is a subsolution and u a supersolution. This implies $u \equiv v$, and the following theorem holds.

Theorem 2.3. *The value function is the unique viscosity solution of the Hamilton–Jacobi–Bellman equation.*

Hence, to find the value function of a dynamic optimization problem, it is sufficient to construct a viscosity solution of the associated Hamilton–Jacobi–Bellman equation. The construction will be effected by glueing together differentiable local solutions of the Hamilton–Jacobi–Bellman equation. In the hedgehog example we have seen that there are restrictions on how to glue local solutions together. The following theorem specifies these restrictions.

Theorem 2.4. *Let* $\hat{x} \in \Omega$, $V(x)$ *a viscosity solution of the Hamilton–Jacobi–Bellman equation, and* $\varphi\colon \Omega \to \mathbb{R}$ *be a continuously differentiable function such that* $\varphi(\hat{x}) = V(\hat{x})$ *and* $\varphi(x) \ge V(x)$ *for* $x \in \Omega$. *Then*

$$rV(\hat{x}) - H(\hat{x}, \varphi'(\hat{x})) = 0.$$

Compare Bardi and Capuzzo-Dolcetta (2008, Theorem 5.6).

To apply the theorem, consider the situation $p \mapsto H(x, p)$ is strictly convex, and that the value function $V(x)$, which is the unique viscosity solution of the Hamilton–Jacobi–Bellman equation, is continuously differentiable in a neighborhood of $\hat{x}$, but that

$$p_- = \lim_{x \uparrow \hat{x}} V'(x) > \lim_{x \downarrow \hat{x}} V'(x) = p_+.$$

That is, the function V has a kink at $\hat{x}$ whose sharp point is pointing upward. If $p^+ < p < p^-$, it is easy to construct a function φ satisfying $\varphi(\hat{x}) = V(\hat{x})$, $\varphi'(\hat{x}) = p$ and $\varphi(x) \geq V(x)$ for all x.

Then Theorem 4. implies, by continuity, that

$$H(\hat{x}, p^-) = H(\hat{x}, p) = H(\hat{x}, p^+),$$

but this violates strict convexity of $p \mapsto H(x, p)$.

Hence if a value function is continuous and has piecewise continuous first derivatives, and the function H is strictly convex in its second argument, the value function satisfies the Hamilton–Jacobi–Bellman equations at points of differentiability and its derivative has to jump upwards at points of non-differentiability.

The following construction theorem states that these conditions are also sufficient.

Theorem 2.5. *Let $V: \bar{\Omega} \to \mathbb{R}$ be continuous and have piecewise continuous first derivatives. Assume that for every point $\hat{x} \in \Omega$, the following holds: if $p_- = \lim_{x \uparrow \hat{x}} V'(x)$ and $p_+ = \lim_{x \downarrow \hat{x}} V'(x)$, then*

$$p_- \leq p_+ \text{ and } H(\hat{x}, p_-) = H(\hat{x}, p_+). \tag{22}$$

Then V is a viscosity solution of the Hamilton–Jacobi–Bellman equation.

Proof. We have to show that V is a viscosity solution of the Hamilton–Jacobi–Bellman equation at points of nondifferentiability.

Let $\hat{x}$ be such a point. There is a neighborhood of $\hat{x}$ such that V is differentiable for all points in the neighborhood, and

$$rV(\hat{x}) - H(\hat{x}, p_-) = \lim_{x \uparrow \hat{x}} [rV(x) - H(x, V'(x))] = 0.$$

Similarly $rV(\hat{x}) - H(\hat{x}, p_+) = 0$.

Let $\varphi : \bar{\Omega} \to \mathbb{R}$ be a continuously differentiable function such that $V(x) \geq \varphi(x)$ for all x and $V(\hat{x}) = \varphi(\hat{x})$, that is, the graph of φ touches the graph of V from below at $\hat{x}$. Necessarily

$$p_- \leq \varphi'(\hat{x}) \leq p_+.$$

By the convexity of $p \mapsto H(\hat{x}, p)$ and the fact that $H(\hat{x}, p_-) = H(\hat{x}, p_+)$, it follows that

$$H(\hat{x}, \varphi'(\hat{x})) \leq H(\hat{x}, p_-).$$

Consequently

$$0 = rV(\hat{x}) - H(\hat{x}, p_-) \geq rV(\hat{x}) - H(\hat{x}, \varphi'(\hat{x})).$$

It follows that V is a viscosity solution at $\hat{x}$. □

3.3 | Costate equation

We shall construct piecewise differentiable functions V that satisfy the Hamilton–Jacobi–Bellman equation at points of differentiability and the jump condition (22) at points of non-differentiability. Consider therefore an open set and a solution V of the Hamilton–Jacobi–Bellman equation that is smooth when restricted to the open set. The aim of this section is to characterize V.

The solution strategy is to differentiate the Hamilton–Jacobi–Bellman equation with respect to the state variable, to obtain an equation that contains only the first and the second derivative of the value function, and that is linear in the second derivative, a so-called quasi-linear equation.

This equation can be analyzed with a dynamical system, the canonical system, that allows to construct the first derivative $p = V'$, or costate, of the value function. If the state space is higher dimensional, p is a vector-valued function whose components have to satisfy an integrability condition: this leads to the theory of symplectic geometry. In the present one-dimensional situation, integrability is automatically satisfied. To obtain the value function from the costate, the value has to be computed at one point in state space. Typically, this is done at steady states, where the objective functional can be evaluated directly.

Differentiating the Hamilton–Jacobi–Bellman equation yields

$$rV'(x) - \frac{\partial H}{\partial x}(x, V'(x)) - \frac{\partial H}{\partial p}(x, V'(x))V''(x) = 0.$$

This is an equation in $p(x) = V'(x)$, the so-called costate equation

$$\frac{\partial H}{\partial p}(x, p)\frac{dp}{dx} = rp - \frac{\partial H}{\partial x}(x, p). \tag{23}$$

By definition, the costate is the marginal increase in value if the state value is increased. For example, for a pollution problem, more pollution means less value, and the costate is typically a negative quantity.

As usual with first-order equations, it is convenient to rewrite this equation as a differential form

$$\left(rp - \frac{\partial H}{\partial x}(x, p)\right)dx - \frac{\partial H}{\partial p}(x, p)dp = 0,$$

and to note that any integral curve $(x(s), p(s))$ has to satisfy

$$\begin{pmatrix} x' \\ p' \end{pmatrix} = \alpha(x,p) \begin{pmatrix} \frac{\partial H}{\partial p}(x,p) \\ rp - \frac{\partial H}{\partial x}(x,p) \end{pmatrix}, \tag{24}$$

where $\alpha(x,p)$ is a real-valued function, only affecting the parametrization of the integral curves.

For a dynamic optimization problem we have

$$\frac{\partial H}{\partial p}(x,p) = f(x,a(p)),$$

where $a(p)$ is the optimal action for the given value of the costate that maximizes $\ell + pf$ on the right-hand side of (12). It follows that if $\alpha \equiv 1$ on the right-hand side of (24), then

$$\frac{dx}{ds} = \frac{\partial H}{\partial p}(x,p) = f(x,a(p)) = \frac{dx}{dt}$$

and consequently $s = t +$ constant: the parameter s that parametrizes the integral curves is, up to an additive constant, equal to the time parameter. We find that trajectories of the *canonical system*

$$\dot{x} = \frac{\partial H}{\partial p}(x,p), \quad \dot{p} = rp - \frac{\partial H}{\partial x}(x,p)$$

are integral curves of the costate equation. Put differently, locally we can characterize the graph of the costate $p(x)$ as an integral curve of the canonical system. This characterization will aid us in deriving properties of the costate function. Of course, the canonical system is the same as the state–costate system that features in the Pontryagin maximum principle. The above derivation shows how these arise naturally also in the "value function" approach.

The problem points of (23) are its singularities, which are the points (x,p) where p' cannot be solved explicitly from the equation. These points are characterized by the equation $\frac{\partial H}{\partial p}(x,p) = 0$. Geometrically, these are all points where the tangent vector $(\dot{x},\dot{p})$ to a trajectory is either zero or vertical, according to whether $\dot{p}$ is zero or not. We introduce this set formally as

$$S = \left\{ (x,p) : \frac{\partial H}{\partial p}(x,p) = 0 \right\}.$$

Since $H(x,p)$ is convex in p, the intersection S_x of S with a line $\{x\} \times \mathbb{R}$ is either a point or a line segment. In both situations, $\frac{\partial H}{\partial p}(x,p)$ is positive below S_x and negative above.

If the tangent vector in a singular point is vertical, and if, when passing through S, the derivative $\dot{x}$ changes sign, then the trajectory "bends back" on itself and cannot represent the graph of a function. Such trajectories can, therefore, be removed from consideration. Therefore, the only possibility for the graph of the costate function $p(x)$ to intersect the singular set S is in points where the tangent vector $(\dot{x},\dot{p})$ is zero, that is, in equilibria of the canonical system.

4 | LAKE MANAGEMENT PROBLEM

This section returns to the lake management problem and sets it up such that it is possible to apply the theory. To do so, some specific information is needed about the system response function that is summarized in the following proposition. Its proof is an exercise in calculus and is left to the reader.

Proposition 3.1. *The lake decay* $g(x) = bx - x^2/(1+x^2)$ *has the following properties.*

(*i*) $g'(x)$ *takes a global minimum* $b - 3\sqrt{3}/8 \approx b - 0.65$ *at* $x = 1/\sqrt{3} \approx 0.58$.
(*ii*) *If* $0 < b < 3\sqrt{3}/8$, *then* $g(x)$ *has two nondegenerate critical points* $0 < x_1^c < x_2^c : x_1^c$ *is a local maximizer and* x_2^c *a local minimizer.*
(*iii*) *For* $b \geq 3\sqrt{3}/8$ *the function* $g(x)$ *is strictly increasing.*
(*iv*) *If* $b > \frac{1}{2}$ *then* $g(x) > 0$ *for all* $x > 0$, *while if* $b < \frac{1}{2}$ *then* $g\left(x_2^c\right) < 0$.

See Figures 2 and 4 for illustrations of decay functions with two critical points. The first and the third statement of the proposition bounds the parameter range of fragile systems, as it implies that there are no critical points if $b > 3\sqrt{3}/8$. The second statement says that at the low critical point x_1^c, the system tips there toward the costly high pollution region, whereas at the high critical point x_2^c it tips back to the low pollution region. The last statement finally states that tipping back is impossible if the lake system is too fragile, that is, if $b < \frac{1}{2}$. Put briefly, there are no physical tipping points in the system if the system is robust, that is, if $b > 3\sqrt{3}/8$, and there is no physical possibility from recovering from a bad tipping event if the system is very fragile, that is, if $b < \frac{1}{2}$.

In the following, attention shall be restricted to the intermediate "reversible" case $b > \frac{1}{2}$: this is the situation where the lake can always be brought back to the unpolluted state $x = 0$ by reducing the inflow to 0.

The control set A is chosen such that both critical values of the system response are in the interior of A, and hence such that the lake can always be brought by management action either in the oligotrophic—nutrient-poor—region $0 < x < x_\ell^c$, or in the eutrophic—nutrient-rich—region $x > x_h^c$. We therefore take $A = [a_\ell, a_h]$ for constants $0 < a_\ell < a_h$ such that $a_\ell < g(x_2^c) < g(x_1^c) < a_h$. Having chosen A, we choose the state space $X = (x_\ell, x_h)$ such that the

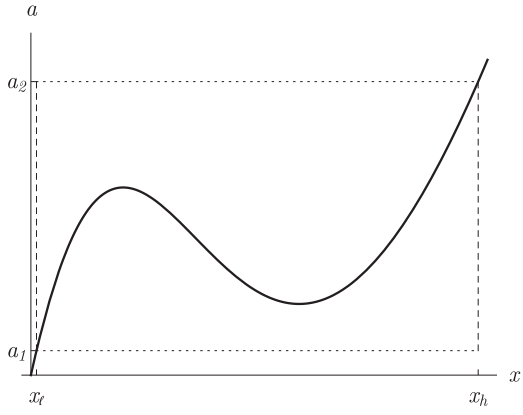

FIGURE 4 State space $X = (x_\ell, x_h)$, action space $A = [a_\ell, a_h]$, and decay function $a = g(x)$

dynamics at the boundary of X are always inward-pointing. Specifically, we choose x_ℓ and x_h such that

$$g(x_\ell) = a_\ell, \quad g(x_h) = a_h \tag{25}$$

—this determines x_ℓ and x_h uniquely—, for in that case

$$f(x_\ell, a) = a - g(x_\ell) \geq 0 \quad \text{and} \tag{26}$$

$$f(x_h, a) = a - g(x_h) \leq 0 \tag{27}$$

for all $a \in A$. Then no action can take the state to the complement of X (see Figure 4).

The function $H(x,p) = \max_{a \in A}[\ell(x,a) + pf(x,a)]$ evaluates to

$$H(x,p) = \Phi(p) - cx^2 - p\left(bx - \frac{x^2}{1+x^2}\right),$$

where Φ is the continuously differentiable function

$$\Phi(p) = \begin{cases} \log a_\ell + pa_\ell, & p \in C_1 = (-\infty, -a_\ell^{-1}], \\ -\log(-p) - 1, & p \in I = (-a_\ell^{-1}, -a_h^{-1}), \\ \log a_h + pa_h, & p \in C_2 = [-a_h^{-1}, \infty), \end{cases} \tag{28}$$

whose derivative $\varphi(p) = \Phi'(p)$ is given as

$$\varphi(p) = \begin{cases} a_\ell, & p \in C_1, \\ -\dfrac{1}{p}, & p \in I, \\ a_h, & p \in C_2. \end{cases} \tag{29}$$

Note for later use that the maximum in the definition of H is taken at $a^* = \varphi(p)$. In particular, if $p \in C_1 \cup C_2$, where C_1 and C_2 are the *corner action* regions, then the maximum is taken in a corner point of A, while if $p \in I$, the *interior action* region, it is taken in an interior point. The graphs of Φ and φ are shown in Figure 5.

The Hamilton–Jacobi–Bellman equation reads as

$$rV(x) - \Phi(V'(x)) + cx^2 + V'(x)g(x) = 0, \tag{30}$$

and the equation for the costate $p(x) = V'(x)$ is

$$(\varphi(p(x)) - g(x))p'(x) = (r + g'(x))p(x) + 2cx. \tag{31}$$

The associated canonical system is

$$\frac{dx}{dt} = \varphi(p) - g(x), \quad \frac{dp}{dt} = (r + g'(x))p + 2cx. \tag{32}$$

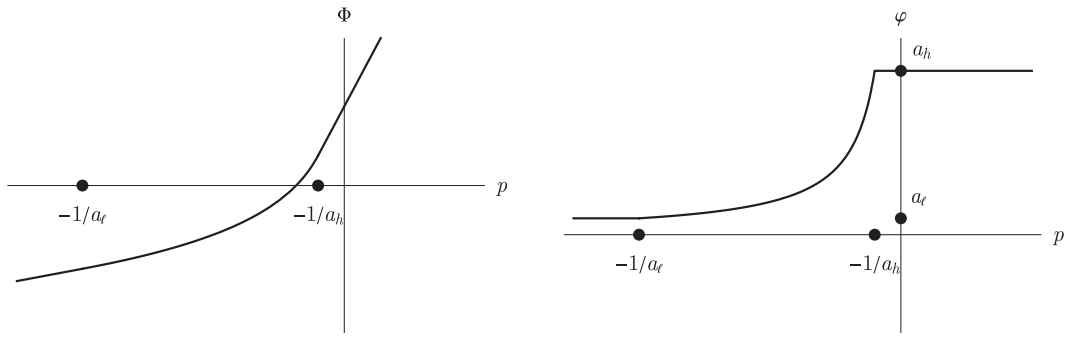

FIGURE 5 Graphs of $\Phi(p)$ and $\varphi(p)$

When interpreting results, it is often convenient to write these equations in terms of the action variable a. This is of course only possible if $p \in I$, as $a = \varphi(p)$ is invertible only there. For the lake, we obtain as state–action system

$$\frac{dx}{dt} = a - g(x), \quad \frac{da}{dt} = -(r + g'(x))a + 2cxa^2, \tag{33}$$

valid for $a(t)$ in the interior of the action space A.

In the following, we shall analyze this system for the fixed discount rate $r = 0.03$, which corresponds to a time horizon of $\log(2)/r \approx 23$ years, that is, approximately one generation. As this value has been widely used, the choice is made mainly to be consistent with the rest of the literature.

4.1 | Steady state analysis

By construction of the state space, all steady states of the state–action system are located in the interior of the product $X \times A$ of state space and action space. The steady states satisfy the two equations

$$a = g(x) \quad \text{and} \quad a = \frac{r + g'(x)}{2cx}, \tag{34}$$

or, equivalently, they are of the form $(x, g(x))$ with x a root of the equation

$$r + g'(x) - 2cxg(x) = 0.$$

Instead of solving this equation for x, which is hard, it is solved for c, which is easy, to obtain

$$c = \Psi(x, b) = \frac{r + g'(x)}{2xg(x)} = \frac{(r + b)(1 + x^2)^2 - 2x}{2x^2(1 + x^2)(b - x + bx^2)}. \tag{35}$$

Plotting the graph of $\Psi(x, b)$ for fixed values of b in a (c, x) diagram, as in Figure 6, shows for each value of c the number of steady states.

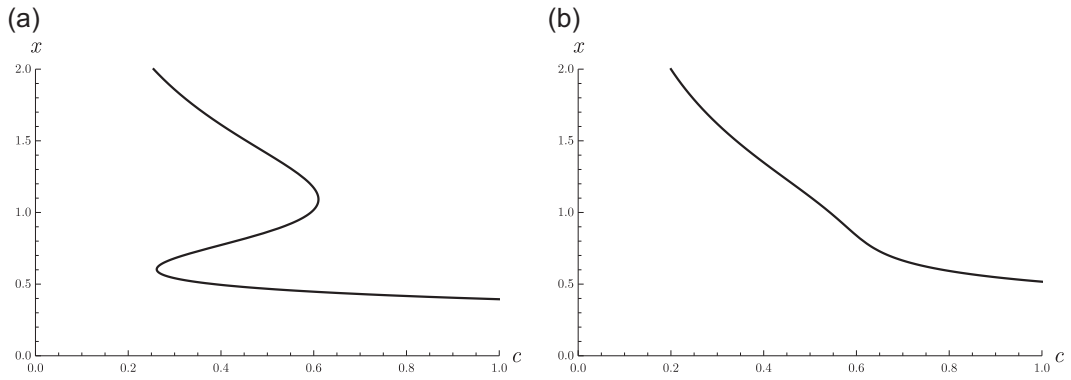

FIGURE 6 Bifurcation diagrams. (a) $b = 0.66$ and (b) $b = 0.85$

The function Ψ not only determines the position of the steady states in the (c, x) diagram, it also determines their type.

Proposition 3.2. *Let $b > \frac{1}{2}$ and $r > 0$. If for a given parameter values (b, c, r) the state–costate system has a steady state $(\bar{x}, \bar{p})$ such that $\frac{\partial \Psi}{\partial x}(\bar{x}, b) < 0$, it is a saddle, while if $\frac{\partial \Psi}{\partial x}(\bar{x}, b) > 0$, it is a repeller.*

It can be shown that a stable steady state $(\bar{x}, \bar{a})$ of the state–action system corresponds to a weak local optimum of the benefit functional: that is, no loading schedule $a(t)$ close to $\bar{a}$ can achieve a better outcome. The proposition characterizes all such locally optimal loading schedules in terms of the function Ψ.

Proof. The derivative of Ψ reads as

$$\frac{\partial \Psi}{\partial x} = \frac{g''(x) - 2c(g(x) + xg'(x))}{2xg(x)}, \tag{36}$$

where $c = \Psi(x)$.

To determine the nature of the steady state, we use the state–action system (33), to obtain the derivative of the vector field at the steady state as

$$\tilde{D} = \begin{pmatrix} -g'(x) & 1 \\ 2ca^2 - ag''(x) & 4cax - (r + g'(x)) \end{pmatrix}.$$

The steady state Equations (34) can be used to replace $r + g'(x)$ by $2cax$ and a by $g(x)$, to yield

$$\tilde{D} = \begin{pmatrix} -g'(x) & 1 \\ g(x)(2cg(x) - g''(x)) & 2cxg(x) \end{pmatrix}. \tag{37}$$

Computing the determinant yields

$$\det \tilde{D} = g(x)(-2cxg'(x) - 2cg(x) + g''(x)) = 2xg(x)^2 \frac{\partial \Psi}{\partial x}.$$

To show the theorem, note that if $\frac{\partial \Psi}{\partial x} < 0$, then the determinant is negative, which implies that the eigenvalues of $\tilde{D}$ are real and have opposite signs. This shows that the steady state is a saddle in this situation.

If $\frac{\partial \Psi}{\partial x} > 0$, the determinant is positive, and the eigenvalues have either both positive real part or both negative real part, so the steady state is either a repeller or an attractor. Now, the type is independent of the coordinates used to represent the system. We, therefore, pass to state–costate coordinates and consider the linearization of the state–costate system at the steady state. This is of the form

$$D = \begin{pmatrix} -g'(x) & \varphi'(x) \\ g''(x)p + 2c & r + g'(x) \end{pmatrix}.$$

As the trace of this matrix is $r > 0$—this is a property of general canonical systems—, we conclude that the sum of the eigenvalues is positive and the steady state is a repeller if $\frac{\partial \Psi}{\partial x} > 0$. This proves the theorem. □

Critical values of $x \mapsto \Psi(x, b)$ correspond to bifurcations of steady states of (32). For instance, if $b = 0.66$ there are two nondegenerate critical points, $(c, x) = (0.26, 0.60)$ and $(0.61, 1.09)$ (see Figure 6a). For $c < 0.26$, there is a single steady state x having values larger than 2. At the critical value, two additional steady states are generated in a saddle-node bifurcation at $x = 0.60$. For $0.26 < c < 1.09$, three steady states exist. At $c = 1.09$ two steady states disappear in another saddle-node bifurcation at $x = 1.09$, and for larger values of c a single steady state remains around $x \approx 0.3$.

If the resilience parameter b is increased, Figure 6b suggests that $\Psi(x, b)$ is eventually monotonically decreasing in x. This means that the two saddle-node bifurcation points have disappeared in a cusp bifurcation, which necessarily occurs at a degenerate critical point.

To make these statements precise, we make use of the fact that $\Psi(x, b)$ is a rational function, the quotient of two polynomials. In the following, we shall need information on the location of roots of polynomials that are derived from Ψ. There are exact algorithms to determine the number of roots of polynomials with rational coefficients in a given interval, which are far-reaching refinements of the well-known Descartes sign rule. They will allow us to formulate global results. These algorithms are too time-consuming to apply by hand, but they are implemented in symbolic computer algebra packages.

Proposition 3.3 (Existence of cusp bifurcation). *If $r = 3/100$, the system (32) has a cusp bifurcation for $(b, c) = (b_{\text{cusp}}, c_{\text{cusp}})$ at x_{cusp}, where $b_{\text{cusp}} \in [771/10^3, 772/10^3]$. Approximately, the bifurcation values of the parameters are $b_{\text{cusp}} \approx 0.771418$, $c_{\text{cusp}} \approx 0.568895$, $x_{\text{cusp}} \approx 0.819681$. This is the only cusp bifurcation point in the parameter region $b > \frac{1}{2}$.*

Recall that Proposition 1. states that if and only if $b < 3\sqrt{3}/8 \approx 0.65$, there are multiple steady states under constant loading in the system, and hence physical tipping points. The present proposition is the economic analogue of this: it states that if and only if $b < b_{\text{cusp}} \approx 0.77$, there are multiple locally optimal steady states in the system. The apparent paradox that this

can happen for values of b for which there are no physical tipping points is resolved by the remark that now time-varying pollution schedules are admitted.

Proof. A once degenerate critical value of $x \mapsto \Psi(x, b)$ is a cusp bifurcation value. That is, if a cusp bifurcation occurs for the parameter values $(\bar{b}, \bar{c})$ at $\bar{x}$, then

$$\bar{c} = \Psi(\bar{x}, \bar{b}), \quad \frac{\partial \Psi}{\partial x}(\bar{x}, \bar{b}) = 0, \quad \text{and} \quad \frac{\partial^2 \Psi}{\partial x^2}(\bar{x}, \bar{b}) = 0. \tag{38}$$

Note that since the denominator of $\Psi(x, b)$ is nonzero for all (x, b) such that $x > 0$ and $b > \frac{1}{2}$, this property is shared with all derivatives of $\Psi(x, b)$.

Writing $\frac{\partial}{\partial x}\Psi(x, b) = F(x, b)/G(x, b)$, with F and G polynomials in x and b, the latter two conditions in (38) are equivalent to $F(\bar{x}, \bar{b}) = 0$, $\frac{\partial}{\partial x}F(\bar{x}, \bar{b}) = 0$, that is, the polynomial $x \mapsto F(x, b)$ has a double root $\bar{x}$. Necessary and sufficient for this is that the discriminant of this polynomial has a root at $b = \bar{b}$ van der Waerden (1955, p. 93). For polynomials with rational coefficients, like in the present case, the number of roots in an arbitrary given interval can be determined exactly by a computer algebra package.

Appendix A shows the code of an implementation and its output. There are three results. First, the discriminant $\Delta(b)$ has a single root in the region $b > 1/2$. Second, the root is approximately located at $b = 0.771419$. Third, the interval $[771/10^3, 772/10^3]$ contains the root, which is the cusp bifurcation value b_{cusp}. The first and third are exact results, which can in principle be replicated by hand.

The values for c_{cusp} and x_{cusp} can be determined similarly exactly, but that is not needed in the following. □

Of course, the interval containing the bifurcation value b_{cusp} can be made as small as desired, and similar intervals can be found for the bifurcation values c_{cusp} and x_{cusp}.

From the theory of cusp bifurcations, it is known that two curves of saddle-node bifurcations in the (b, c) plane emerge from the cusp bifurcation point.

Proposition 3.4 (Saddle-node bifurcations). *For $b > b_{\text{cusp}}$, the system has a single steady state for all values of $c > 0$.*

For $b \in \left(\frac{1}{2}, b_{\text{cusp}}\right)$, there is a family of saddle-node bifurcation values $c^1_{\text{SN}}(b) < c^2_{\text{SN}}(b)$, $i = 1, 2$, such that the system has three steady states with positive values of x if $c \in \left(c^1_{\text{SN}}(b), c^2_{\text{SN}}(b)\right)$ and one if $c \in \left(0, c^1_{\text{SN}}(b)\right) \cup \left(c^2_{\text{SN}}(b), \infty\right)$.

Moreover, $c^1_{\text{SN}}(b) < 0$ for $b \in \left(\frac{1}{2}, 3\sqrt{3}/8 - 3/100\right)$ and $c^1_{\text{SN}}(b) > 0$ for $b \in (3\sqrt{3}/8 - 3/100, b_{\text{cusp}})$, and $c^1_{\text{SN}}(b_{\text{cusp}}) = c^2_{\text{SN}}(b_{\text{cusp}})$.

This proposition sharpens the result of Proposition 3. by giving tight restrictions on the set of parameter values for which there are multiple locally optimal states in the lake system. Geometrically, it has the shape of a wedge with vertex at $(b_{\text{cusp}}, c_{\text{cusp}})$, and with the graph of $c^1_{\text{SN}}(b)$ as its lower edge and $c^2_{\text{SN}}(b)$ as its upper edge.

Proof. Retaining the definitions of F and G from the proof of the previous proposition, by using a computer algebra package it is readily shown that $F(x, 1)$ does not have a root

in the interval $x > 0$. Hence the function $\Psi(x, 1)$ is monotonically decreasing. If there were a value $\hat{b} > b_{\text{cusp}}$ such that $\Psi(x, \hat{b})$ is not monotonically decreasing, by changing b from 1 to $\hat{b}$, there is necessarily an intermediate value $\tilde{b} > b_{\text{cusp}}$ such that $\frac{\partial \Psi}{\partial x}(x, \tilde{b})$ has a double root for some x. This would be a degenerate critical point. But we know already that no such point exists for $b > b_{\text{cusp}}$, hence $\hat{b}$ cannot exist and $x \mapsto \Psi(x, b)$ is monotonically decreasing whenever $b > b_{\text{cusp}}$.

Similarly, in the region $\frac{1}{2} < b < b_{\text{cusp}}$ there are for any fixed value of b the same number of saddle-node bifurcations. For $b = 6/10$, this number is established to be 2. Hence there are two saddle-node curves that can be written as the graph of a function $c = c^i_{\text{SN}}(b)$.

Finally, solving the equations $\Psi(x, b) = 0$, $\frac{\partial \Psi}{\partial x}(x, b) = 0$ yields that there is a critical value $c = 0$ for $b = 3\sqrt{3}/8 - 3/100$ and $x = \sqrt{3}/3$. This shows the final line of the theorem. □

4.2 | Analysis of state–costate system: One steady state

Proposition 4. implies that for $r = 3/100$ and $b \in \left(\frac{1}{2}, b_{\text{cusp}}\right)$, there are at most three interior steady states of the state–costate system (32), or, equivalently, of the state–action system (33), while for $b \in (b_{\text{cusp}}, \infty)$, there is only one.

This section constructs in the first situation solutions to the state–costate system that give rise to a viscosity solution of the Hamilton–Jacobi equation.

If the state–costate system (32) has a single saddle steady state, the Hamilton–Jacobi–Bellman equation has a differentiable solution, which is the stable manifold of the saddle. Recall that the stable manifold $\bar{z} = (\bar{x}, \bar{p})$ is the set of all points z_0 such that the state–costate trajectory starting in z_0 tends to $\bar{z}$ as $t \to \infty$. By the Invariant Manifold Theorem (Guckenheimer & Holmes, 1986; Hirsch, Pugh, & Shub, 1977), the stable manifold of a saddle in a two-dimensional system is a smooth curve.

Proposition 3.5. *Let $b > \frac{1}{2}$, $r > 0$ and $c > 0$ be fixed such that $c = \Psi(x, b)$ has a single solution $\bar{x}$ such that $\frac{\partial \Psi}{\partial x}(\bar{x}, b) < 0$. Then the Hamilton–Jacobi–Bellman equation has a smooth solution $V(x)$, which is the value function.*

This proposition is remarkable, as it gives a local criterium, in terms of the function Ψ, for the global solvability of dynamic optimization problem. The optimal management schedule steers the system from any initial state toward the steady state $\bar{x}$.

Proof. By the hypothesis and Proposition 2., the unique steady state of the state–costate system $(\bar{x}, \bar{p})$ with $\bar{p} = -1/g(\bar{x})$ is a saddle.

From (37) we see that the vector $(0, 1)$ cannot be an eigenvector of the matrix $\tilde{D}$. Then by the Invariant Manifold Theorem, locally around the steady state, the stable manifold of the saddle can be written as the graph of a function $a = \tilde{w}^s(x)$, or, equivalently, of a function $p = w^s(x)$. We extend the stable manifold by integrating the local manifold backwards in time.

The set

$$B = \{(x, a): (0 < x < \bar{x} \quad \text{and} \quad -1/g(x) < p < 0) \\ \text{or} \quad (x > \bar{x} \quad \text{and} \quad p < -1/g(x))\},$$

the shaded set in Figure 7, is a backward trapping region: it is readily verified that on its boundary, all vectors are either tangent or outward pointing. Hence trajectories $(x(t), a(t))$ on the stable manifold can never leave B as $t \to -\infty$. In particular, the trajectories cannot cross the curve $\dot{x} = a - g(x) = 0$. Hence $x(t)$ is monotonically increasing, if $x(t) < \bar{x}$, or decreasing, if $x(t) > \bar{x}$, and the trajectory can be represented as the graph of a curve $a = \tilde{w}^s(x)$ for all $x \in X$.

By construction, the function $p(x) = w^s(x)$ solves the costate Equation (31). The corresponding value function can be determined in two different manners. Either the function $w^s(x)$ is integrated, taking into account that at the steady state the integral $J(\bar{x}, \bar{a})$, where $\bar{a} = -1/w^s(\bar{x})$, can be computed directly. Or it is determined directly from the Hamilton–Jacobi–Bellman Equation (30) as

$$V(x) = \frac{1}{r}H(x, w^s(x)) = \frac{1}{r}(\varphi(w^s(x)) - cx^2 + w^s(x)g(x)). \tag{39}$$

Either way, the resulting function $V(x)$ is a smooth solution of the Hamilton–Jacobi–Bellman equation, hence the unique viscosity solution, and therefore equal to the value function. Finally

$$a^*(x) = \varphi'(w^s(x))$$

is the optimal action schedule in feedback form. □

4.3 | Analysis of state–costate system: Three steady states

If the state–costate system has three steady states, then two of these have to be saddles. The stable manifolds of either of these saddles are then candidates for being the graph of the costate function. We, therefore, have to compare their values.

There are three configurations of the relative positions of the two stable manifolds, one of which will be seen to be impossible on theoretical grounds. The first is that the stable manifold of one of the saddles is the graph of a function, that is, defined on the complete state space (Figure 8).

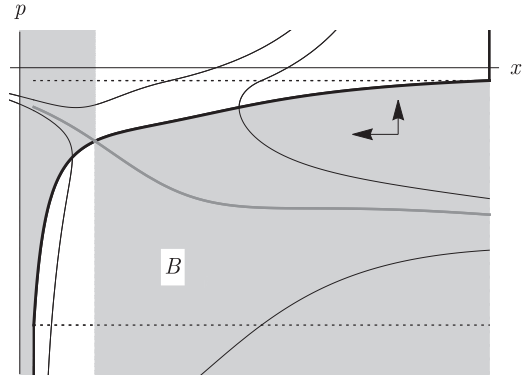

FIGURE 7 Backward trapping region B

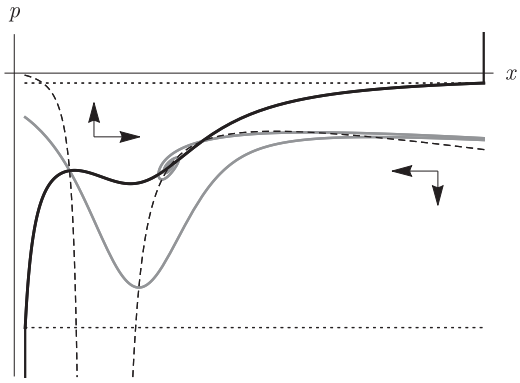

FIGURE 8 Configurations of relative positions of stable manifolds when $w_1^s(x)$ is defined globally. Shown are the curves $\dot{x} = 0$ (solid black), $\dot{p} = 0$ (dashed), the stable manifolds W_1^s and W_2^s (gray), and the boundaries of the interior action region I (dotted)

The second, which will be shown to be impossible, is that both stable manifolds define graphs of functions that are defined on the complete state space (Figure 9).

The last configuration is that locally both stable manifolds are described by functions defined on a subinterval of the state space; these subintervals may overlap (Figure 10).

In the first configuration, where a stable manifold is equal to the graph of a function $w_i^s: X \to \mathbb{R}$, this gives rise to a smooth solution $V(x)$ of the Hamilton–Jacobi–Bellman equation in the same manner as in the one steady state case: see Equation (39).

To see that the second configuration is impossible, we need the following auxiliary result. A *region* in the plane will denote an open set R whose boundary ∂R is a piecewise differentiable curve. It is *forward invariant* under a dynamical system if every forward orbit with an initial point in the closure $\bar{R}$ of R is contained in $\bar{R}$.

Lemma 3.1. *Let $r > 0$. A continuous time dynamical system in a planar region defined by the state–costate equations*

$$\dot{x} = \frac{\partial H}{\partial p}, \quad \dot{p} = rp - \frac{\partial H}{\partial x}$$

cannot have a bounded nonempty forward invariant subregion of positive area.

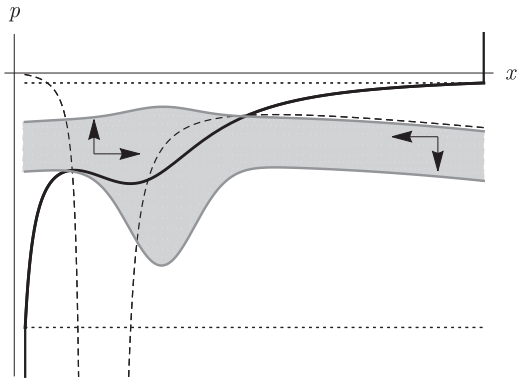

FIGURE 9 Impossible configuration. Curves as in Figure 8

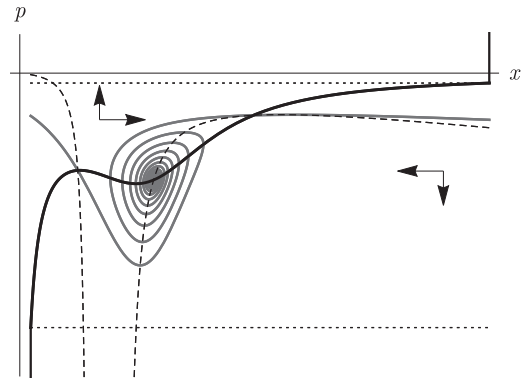

FIGURE 10 $w_1^s(x)$ and $w_2^s(x)$ defined locally. Curves as in Figure 8

Proof. Let $F(x,p) = \left(\frac{\partial H}{\partial p}, rp - \frac{\partial H}{\partial x}\right)$ be the vector field defined by the right-hand side of the state–costate equations.

Assume, by contradiction, that R is a forward invariant subregion whose area is positive. Denote the boundary of R by ∂R. As the boundary is piecewise differentiable, for all but finitely many boundary points $(x,p) \in \partial R$, there is a unique outward pointing normal vector $n(x,p)$. Since R is forward invariant, $F \cdot n \leq 0$ whenever n is defined.

By the divergence theorem, the area integral of div F over R equals the line integral of $F \cdot n$ over ∂R,

$$\iint_R \mathrm{div} F dA = \int_{\partial R} F \cdot n dL. \tag{40}$$

As R is forward invariant, the line integral evaluates to a quantity smaller than or equal to 0. The integrand of the surface integral is, however, larger than 0, as

$$\mathrm{div} F = \frac{\partial}{\partial x}\frac{\partial H}{\partial p} + \frac{\partial}{\partial p}\left(rp - \frac{\partial H}{\partial x}\right) = r > 0, \tag{41}$$

which yields a contradiction. □

Assuming that the second configuration is possible, let $\bar{x}_1 < \bar{x}_2$ denote the state coordinate of the two saddle steady states, and assume that $w_1^s, w_2^s : X \to \mathbb{R}$ parametrize the stable manifolds of the two saddle equilibrium points. These manifolds cannot intersect, and as $w_1^s(x) < w_2^s(x)$ if $\bar{x}_1 < x < \bar{x}_2$, the former inequality holds for all $x \in X$. The set

$$F = \{(x,p) \in X \times \mathbb{R} : w_1^s(x) < p < w_2^s(x)\}$$

is open, bounded and forward invariant. But this contradicts the lemma.

We shall show that the third configuration may give rise to a viscosity solution of the Hamilton–Jacobi–Bellman equation that is not a smooth solution. Actually, there is only a single point at which differentiability of the value function breaks down. This point turns out to be an *indifference point*, at which two different admissible action schedules give rise to the same optimal payoff.

Proposition 3.6. *Let $b > \frac{1}{2}$, $r > 0$ and $c > 0$ be fixed such that the state–costate equations have two saddle steady states $(\bar{x}_1, \bar{p}_1)$ and $(\bar{x}_2, \bar{p}_2)$ and one repeller $(\bar{x}_3, \bar{p}_3)$. Let D_1, $D_2 \subset X$ be the closures relative to X of the maximal domains of definition of continuous functions $w_i^s : D_i \to \mathbb{R}$ such that the graph of w_i^s is a subset of the stable manifold W_i^s of the steady state $(\bar{x}_i, \bar{p}_i)$.*

Assume that neither D_1 nor D_2 is equal to X. Then the intersection $\bar{D} = D_1 \cap D_2$ of D_1 and D_2 is nonempty.

Moreover, if $\bar{D}$ contains only a single point, then the Hamilton–Jacobi–Bellman equation has a smooth solution. If $\bar{D}$ is an interval of nonzero length, then the Hamilton–Jacobi–Bellman equation has a continuous but nondifferentiable viscosity solution, and $\bar{D}$ contains an indifference point.

This proposition characterizes the situation that there are two strongly optimal locally stable steady states. Here "strong" refers to the fact that all possible pollution schedules $a(t)$ are admitted, not only those with values close to the steady state value. The indifference point separates two very different economic regimes: the one going to the low pollution steady state is characterized by large negative values of the costate $p(x) = V'(x)$, hence a high incentive to reduce pollution through low loadings. The optimal management policy is characterized by a conservational approach and larger long-time benefits. The other economic regime is the one that steers the system to a high pollution steady state. That one is characterized by small negative values of the costate, and low incentives to contain pollution. The policy is an industry-first approach that generates short-time benefits and larger long-time costs.

Proof. We have to investigate the various possible geometrical configurations of the stable manifolds. For the part of the stable manifold extending from the left-hand saddle point $(\bar{x}_1, \bar{p}_1)$ in the direction of increasing values of the state variable, these are illustrated in Figure 11.

Each orbit $(x(t), p(t))$ on this stable manifold locally parametrizes the manifold and accumulates on the saddle point for $t \to \infty$. We shall classify the possible behavior of the orbit as t decreases.

By the Poincaré–Bendixson theorem, the distance of $(x(t), p(t))$ either increases to infinity as $t \to -\infty$, or it accumulates on a steady state, or on an invariant cycle.

Cycles are ruled out by lemma 1.

Orbits tending to infinity but not intersecting the half-line $L = \{(x, p) : x = \bar{x}_2,\ p < \bar{p}_2\}$—curves *i* and *ii* in the figure—can be ruled out as follows.

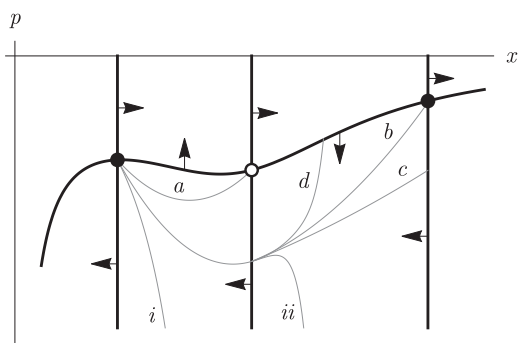

FIGURE 11 Sketch of possible configurations of the stable manifold of the saddle $(\bar{x}_1, \bar{p}_1)$. Black dots indicate saddle steady states, the white dot indicates the repeller. The black curve is the locus $\dot{x} = 0$

If there were such an orbit, there is $T < 0$ such that $p(t) < -1/a_\ell$ for all $t < T$. For these values of t, the state equation reads as $\dot{x}(t) = a_\ell - g(x(t))$. But in the region R_1, the value of $g(x)$ is bounded away from a_ℓ, say $g(x) \geq a_\ell + \varepsilon$ for some $\varepsilon > 0$. It follows that $\dot{x} \leq -\varepsilon$, which implies that $x(t_1) \geq \bar{x}_3$ for some $t_1 < T$ and the orbit intersects the half-line L, contrary to assumption.

This leaves us with four possibilities, which are indicated in Figure 11: (1a) the orbit accumulates on the repeller; (1b) it accumulates on the right-hand saddle; (1c) it intersects the half-line L; (1d) it intersects the graph of the function $p = -1/g(x)$ between the lines $x = \bar{x}_3$ and $x = \bar{x}_2$. Analogously, there are four possibilities for the stable manifold of the right-hand saddle: (2a) it accumulates on the repeller; (2b) it intersects the graph of $-1/g(x)$ between the lines $x = \bar{x}_1$ and $x = \bar{x}_3$; (2c) it accumulates on the left-hand saddle; (2d) it intersects the half-line $x = \bar{x}_1$, $p > \bar{p}_1$. Again, the impossibility of the state–costate dynamics having compact invariant regions rules out the possibilities that (1b) or (1c) obtain simultaneously with either (2b) or (2c).

If (1a) and (2a) both obtain, then the union of the two stable manifolds form the graph of a continuous function, which implies that the Hamilton–Jacobi–Bellman equation has a smooth solution.

If (1c) obtains, the stable manifold of the left-hand saddle, together with the part of the stable manifold of the right-hand saddle that is located in the region $x > \bar{x}_3$ form the graph of a continuous function, again implying that the Hamilton–Jacobi–Bellman equation has a smooth solution. An analogous argument holds if (2c) obtains.

If either (1d) or (2d) obtains, the stable manifold of respectively the left or the right-hand saddle can be extended to a function defined on all of X, contrary to assumption. Finally, consider the situation that (1b) obtains, together with either (2a) or (2b). In that case, the closure relative to X of the maximal domain of definition of the function w_1^s parametrizing the part of the stable manifold of the left-hand saddle that contains the saddle is of the form $D_1 = (x_\ell, d_{h,1}]$, with $\bar{x}_3 < d_{h,1} < \bar{x}_2$. The analogous set is of the form $D_2 = [d_{\ell,2}, x_h)$ with $d_{\ell,2} = \bar{x}_3$ if (2a) obtains and $\bar{x}_1 < d_{\ell,2} < \bar{x}_3$ if (2b) obtains. In particular, the intersection

$$\bar{D} = D_1 \cap D_2 = [d_{\ell,2}, d_{\ell,1}]$$

has nonzero length.

For $i = 1, 2$, let the local value functions V_i: $D_i \to \mathbb{R}$ be given as

$$V_i(x) = \frac{1}{r} H(x, w_i^s(x)), \quad x \in D_i.$$

Since $p \mapsto H(x, p)$ is convex, it takes its minimum at the critical point $p = -1/g(x)$, whence

$$V_2(d_{\ell,2}) < V_1(d_{\ell,2}) \quad \text{and} \quad V_1(d_{h,1}) < V_2(d_{h,1}).$$

Moreover, since $w_i^s(x) = V_i'(x)$ for $i = 1, 2$ and $w_1^s(x) < -1/g(x) < w_2^s(x)$ for x in the interior of $\bar{D}$, we have that the difference

$$\Delta(x) = V_2(x) - V_1(x)$$

satisfies $\Delta(d_{\ell,2}) < 0 < \Delta(d_{h,1})$ and $\Delta'(x) > 0$ for all $d_{\ell,2} < x < d_{h,1}$. Hence it has a unique zero $\hat{x}$ in the interior of $\bar{D}$. Moreover

$$\lim_{x \uparrow \hat{x}} V_1'(x) = w_1^s(\hat{x}) < w_2^s(\hat{x}) = \lim_{x \downarrow \hat{x}}.$$

By Theorem 5. the function $V : X \to \mathbb{R}$ defined as $V(x) = V_1(x)$ for $x_\ell < x \leq \hat{x}$ and $V(x) = V_2(x)$ for $\hat{x} < x < x_h$ is a viscosity solution of the Hamilton–Jacobi–Bellman equation, and $\hat{x}$ is the indifference point. □

4.4 | Multiple actors

In this article, I have looked only at the single-actor situation. The main reason for this is that the multi-actor problem is not yet theoretically fully resolved. In Mäler et al. (2003) the situation that several decision makers affecting the pollution stock of a single lake by a pollution schedule conditioned on time—the so-called open loop information structure—has been analyzed. Largely, the analysis can be reduced to the single-actor situation, but with the cost, parameter c replaced by c/n, where n is the number of players. The more interesting feedback information structure, where the pollution schedule can be conditioned on the state, has been investigated in Dockner and Wagener (2014). There a "game" Hamilton–Jacobi–Bellman equation has been derived for the value function, which has again the same structure as the single-actor equation. The implications for the dynamics are different, however. The jump in the costate value can occur even if there is only a single long-time steady state. Moreover, there are other, non-viscosity, solutions to the game Hamilton–Jacobi–Bellman equation that correspond to reasonable descriptions of the actors' behavior.

5 | LITERATURE

That optimal management problems may have nondifferentiable value functions became widely known when Skiba published his article on poverty traps (Skiba, 1978), although the insight was obtained by several researchers around the same time (Dechert & Nishimura, 1983; Sethi, 1977). Examples have been described in the context of environmental economics (Brock & Starrett, 2003; Finnoff, Potapov, & Lewis, 2010; Grass, Xepapadeas, & de Zeeuw, 2017; Greiner & Semmler, 2005; Kiseleva & Wagener, 2010, 2015; Kossioris, Plexousakis, Xepapadeas, & de Zeeuw, 2011, 2008; Mäler et al., 2003; Tahvonen & Salo, 1996; Wagener, 2003), industrial organization (Hartl, Kort, Feichtinger, & Wirl, 2004; Haunschmied, Kort, Hartl, & Feichtinger, 2003; Hinloopen, Smrkolj, & Wagener, 2013, 2017; Smrkolj & Wagener, 2019; Wagener, 2005), addiction (Caulkins et al., 2013) political economy (Caulkins, Hartl, Tragler, & Feichtinger, 2001), law enforcement and corruption (Caulkins et al., 2013; Feichtinger & Tragler, 2002), and migration (Caulkins, Feichtinger, Johnson, Tragler, & Yegorov, 2005).

Bifurcation theory can be used to classify different kinds of optimal management policies of the lake model (Kiseleva & Wagener, 2010, 2015; Wagener, 2003). Kossioris and Zohios (2012) were the first to use viscosity techniques to determine the value function in the lake model. Bartaloni (2016) showed the existence of the value function for the lake model with direct methods, which turned out to be a remarkably difficult problem.

ACKNOWLEDGMENT

I gratefully acknowledge the invitation to hold the tutorial lecture "Geometry and the Economic Impact of Ecological Systems with Tipping Points," at the 2019 World Conference on Natural Resource Modelling in Montréal, Canada, and the hospitality of GERAD during my stay.

AUTHOR CONTRIBUTION

F. W. conceived the article, drafted it, gave final approval of the version to be published and agrees to be accountable for all aspects of the work in ensuring that questions related to the accuracy or integrity of any part of the work are appropriately investigated and resolved.

ORCID

Florian Wagener http://orcid.org/0000-0001-6671-8814

REFERENCES

Bardi, M., & Capuzzo-Dolcetta, I. (2008). *Optimal control and viscosity solutions of Hamilton-Jacobi-Bellman equations*. Boston, MA: Birkhäuser.

Bartaloni, F. (2016). Existence of the optimum for shallow lake type models. Preprint, arXiv:1606.06318.

Brock, W. A., & Starrett, D. (2003). Managing systems with non-convex positive feedback. *Environmental and Resource Economics*, 26(4), 575–602.

Carpenter, S. R., & Cottingham, K. L. (1997). Resilience and restoration of lakes. *Conservation Ecology*, 1(2).

Caulkins, J. P., Feichtinger, G., Grass, D., Hartl, R. F., Kort, P. M., Novak, A. J., & Seidl, A. (2013). Leading bureaucracies to the tipping point: An alternative model of multiple stable equilibrium levels of corruption. *European Journal of Operational Research*, 225(3), 541–546.

Caulkins, J. P., Feichtinger, G., Hartl, R. F., Kort, P. M., Novak, A. J., & Seidl, A. (2013). Multiple equilibria and indifference-threshold points in a rational addiction model. *Central European Journal of Operational Research*, 21(3), 507–522.

Caulkins, J. P., Feichtinger, G., Johnson, M., Tragler, G., & Yegorov, Y. (2005). Skiba thresholds in a model of controlled migration. *Journal of Economic Behavior & Organization*, 57(4), 490–508.

Caulkins, J. P., Hartl, R. F., Tragler, G., & Feichtinger, G. (2001). Why politics makes strange bedfellows: Dynamic model with DNS curves. *Journal of Optimization Theory and Applications*, 111(2), 237–254.

Crandall, M. G., & Lions, P. L. (1983). Viscosity solutions of Hamilton-Jacobi equations. *Transactions of the American Mathematical Society*, 277(1), 1–42.

Dechert, W. D., & Nishimura, K. (1983). A complete characterization of optimal growth paths in an aggregated model with a non-concave production function. *Journal of Economic Theory*, 31, 332–354.

Dockner, E. J., & Wagener, F. O. O. (2014). Markov-perfect Nash equilibria in models with a single capital stock. *Economic Theory*, 56, 585–625.

Feichtinger, G., & Tragler, G. (2002). Skiba thresholds in optimal control of illicit drug use. In G. Zaccour (Ed.), *Optimal control and differential games: Essays in honor of Steffen Jørgensen* (pp. 3–21). New York: Kluwer.

Finnoff, D., Potapov, A., & Lewis, M. A. (2010). Control and the management of a spreading invader. *Resource and Energy Economics*, 32(4), 534–550.

Grass, D., Xepapadeas, A., & de Zeeuw, A. (2017). Optimal management of ecosystem services with pollution traps: The lake model revisited. *Journal of the Association of Environmental and Resource Economists*, 4(4), 1121–1154.

Greiner, A., & Semmler, W. (2005). Economic growth and global warming: A model of multiple equilibria and thresholds. *Journal of Economic Behavior & Organization*, 57, 430–447.

Guckenheimer, J., & Holmes, P. (1986). *Nonlinear oscillations, dynamical systems, and bifurcations of vector fields*. New York: Springer.

Hartl, R. F., Kort, P. M., Feichtinger, G., & Wirl, F. (2004). Multiple equilibria and thresholds due to relative investment costs. *Journal of Optimization Theory and Applications*, 123(1), 49–82.

Haunschmied, J. L., Kort, P. M., Hartl, R. F., & Feichtinger, G. (2003). A DNS-curve in a two-state capital accumulation model: A numerical analysis. *Journal of Economic Dynamics and Control*, 27(4), 701–716.

Hinloopen, J., Smrkolj, G., & Wagener, F. O. O. (2013). From mind to market: A global, dynamic analysis of R&D. *Journal of Economic Dynamics and Control*, 37(12), 2729–2754.

Hinloopen, J., Smrkolj, G., & Wagener, F. O. O. (2017). Research and development cooperatives and market collusion: A global dynamic approach. *Journal of Optimization Theory and Applications*, 174(2), 567–612.

Hirsch, M. W., Pugh, C. C., & Shub, M. (1977). *Invariant manifolds*. Heidelberg: Springer.

Kiseleva, T., & Wagener, F. O. O. (2010). Bifurcations of one-dimensional optimal vector fields in the shallow lake system. *Journal of Economic Dynamics and Control*, 34, 825–843.

Kiseleva, T., & Wagener, F. O. O. (2015). Bifurcations of optimal vector fields. *Mathematics of Operations Research*, 40(1), 24–55.

Kossioris, G., Plexousakis, M., Xepapadeas, A., & de Zeeuw, A. (2011). On the optimal taxation of common-pool resources. *Journal of Economic Dynamics and Control*, 35, 1868–1879.

Kossioris, G., Plexousakis, M., Xepapadeas, A., de Zeeuw, A., & Mäler, K.-G. (2008). Feedback Nash equilibria for non -linear differential games in pollution control. *Journal of Economic Dynamics and Control*, 32, 1312–1331.

Kossioris, G., & Zohios, Ch. (2012). The value function of the shallow lake problem as a viscosity solution of a HJB equation. *Quarterly of Applied Mathematics*, 70(4), 625–657.

Mäler, K. G., Xepapadeas, A., & de Zeeuw, A. (2003). The economics of shallow lakes. *Environmental and Resource Economics*, 26(4), 105–126.

Poincaré, H. (1881). Mémoire sur les courbes définies par une équation differentielle (I). *Journal de Mathématiques Pures et Appliquées, Third series*, 7, 375–422.

Poincaré, H. (1882). Mémoire sur les courbes définies par une équation differentielle (II). *Journal de Mathématiques Pures et Appliquées, Third series*, 8, 251–296.

Poincaré, H. (1885). Sur les courbes définies par une équation differentielle (III). *Journal de Mathématiques Pures et Appliquées, Fourth series*, 1, 167–244.

Poincaré, H. (1886). Sur les courbes définies par une équation differentielle (IV). *Journal de Mathématiques Pures et Appliquées, Fourth series*, 2, 151–218.

Sethi, S. P. (1977). Nearest feasible paths in optimal control problems: Theory, examples, and counterexamples. *Journal of Optimization Theory and Applications*, 23(4), 563–579.

Skiba, A. K. (1978). Optimal growth with a convex-concave production function. *Econometrica*, 46, 527–539.

Smrkolj, G., & Wagener, F. O. O. (2019). Research among copycats: R&D, spillovers, and feedback strategies. *International Journal of Industrial Organization*, 65, 82–120.

Tahvonen, O., & Salo, S. (1996). Nonconvexities in optimal pollution accumulation. *Journal of Environmental Economics and Management*, 31(2), 160–177.

van der Waerden, B. L. (1955). *Algebra I* (4th ed.). Springer.

Wagener, F. O. O. (2003). Skiba points and heteroclinic bifurcations, with applications to the shallow lake system. *Journal of Economic Dynamics and Control*, 27, 1533–1561.

Wagener, F. O. O. (2005). Structural analysis of optimal investment for firms with non-concave revenue. *Journal of Economic Behavior & Organization*, 57(4), 474–489.

How to cite this article: Wagener F. Geometrical methods for analyzing the optimal management of tipping point dynamics. *Nat Resour Model*. 2020;e12258. https://doi.org/10.1111/nrm.12258

APPENDIX A: DETERMINATION OF CUSP BIFURCATION POINT

The computer algebra part of the proof of Proposition 3.3 has been programmed in Mathematica. The code and its output are given below.

```
(* Problem data *)

r    = 3/100;
g    = b x-x^2/(1+x^2);
dg   = D[g,x]//Simplify;
Psi  = (dg+r)/(2x g);
dPsi = Simplify[D[Psi,x]];

F    = Numerator[dPsi];

(* At a cusp bifurcation F(.,b) has a double zero *)

disc = Discriminant[F,x];
Print["\nNumber of zeros of the discriminant Disc(F)
       for b >= 1/2 : ", CountRoots[disc,{b,1/2,Infinity}]]

(* Numerical approximation of cusp bifurcation value *)

allSol  = b/.NSolve[disc==0,b];
realSol = Cases[allSol,_?(FreeQ[N[#,16],Complex]&)];
posSol  = Cases[realSol,_?(#>1/2&)];
Print["Numerical approximation of cusp bifurcation values of
       b: ", posSol[[1]] ];

(* Check numerical result *)

Print["Number of roots in the interval [771,418/1,000,000,
771,419/1,000,000] : ",
CountRoots[disc, {b,771418/1000000, 771419/1000000}] ];

(* Numerical approximation of cups bifurcation point *)

{bbar, cbar, xbar} = {b, c, x} /.
   FindRoot[{c == Psi, 0 == F, 0 == dF},
            {{c, 1}, {x, 1}, {b, 77/100}}];
Print["The cusp bifurcation occurs approximately for\n\t
       (b,c) = (", bbar, ",", cbar, ") at x = ", xbar]
```

The output of the programme:

```
Number of zeros of the discriminant Disc(F) for b >= 1/2 : 1
Numerical approximation of cusp bifurcation values of b: 0.771419
Number of roots in the interval
    [771,418/1,000,000, 771,419/1,000,000] : 1
The cusp bifurcation occurs approximately for
    (b,c) = (0.771419,0.568895) at x = 0.819681
```